AIAA JOURNAL
Vol. 45, No. 6, June 2007

Higher-Order Theory for Buckling of Functionally Graded Circular Plates

M. M. Najafizadeh* and H. R. Heydari
Islamic Azan University, 38135/567 Arak, Iran

DOI: 10.2514/1.12146

In this research, mechanical buckling of circular plates composed of functionally graded materials is considered. Equilibrium and stability equations of a functionally graded material circular plate under uniform radial compression are derived, based on the higher-order shear deformation plate theory. Assuming that the material properties vary as a power form of the thickness coordinate variable z and using the variational method, the system of fundamental partial differential equations is established. A buckling analysis of a functionally graded circular plate under uniform radial compression is carried out and the results are given in closed-form solutions. The results are compared with the buckling loads of plates obtained for a functionally graded circular plate based on the first-order shear deformation plate theory and classical plate theory given in the literature. The study concludes that higher-order shear deformation plate theory accurately predicts the behavior of a functionally graded circular plate, whereas the first-order shear deformation plate theory and classical plate theory overestimate buckling loads.

Nomenclature

a	=	radius of plate
E	=	Young's modulus
E_c	=	modulus of ceramic
E_m	=	modulus of metal
h	=	plate thickness
M	=	bending moment
N	=	in-plane force
p_r	=	uniform radial compression
r	=	radial coordinate
u, v	=	radial and transverse displacements, respectively
z	=	thickness coordinate

Introduction

IN RECENT years, studies on new performance materials have addressed new materials known as functionally graded materials (FGMs). These are high-performance, heat-resistant materials that are able to withstand ultrahigh temperature and extremely large thermal gradients used in aerospace industries. FGMs are microscopically inhomogeneous materials in which the mechanical properties vary smoothly and continuously from one surface to the other [1,2]. Typically, these materials are made from a mixture of ceramic and metal. It is apparent from the literature survey that most research on FGMs has been restricted to thermal stress analysis, fracture mechanics, vibration, and optimization. Generally, there are two ways to model the material property gradation in solids: 1) assume a profile for volume fractions [3] and 2) use a micromechanics approach to study the nonhomogeneous media [4]. For composition-profile modeling, polynomial representations including quadratic [5] variations are used. At the microstructural level, a FGM is characterized by transition from a dispersion phase to an alternative structure, with a network structure in between. Nan et al. [6] directly addressed the constitutive relations of FGM and used an analytical approach to describe the uncoupled thermomechanical properties of metal/ceramic FGM. These novel materials were first introduced by Koizumi [7] and then rapidly developed.

The nonlinear equilibrium equations and associated linear stability equations were expressed for bars, plates, and shells by Brush and Almroth in 1975 [8]. The subject matter of this book is the buckling behavior of structural members subjected to mechanical loads. Subsequently, many researchers developed equilibrium and stability equations for plates and shells made of composite layered materials and used them to determine the buckling and vibration behavior of structures. A review of recent developments in laminated composite plate buckling was carried out by Leissa [9]. Considerable research has focused on the buckling analysis of composite plates under mechanical and thermal loads, based on the classical plate theory (CPT) [10–12]. Using the classical plate theory, which neglects the effects of transverse shear deformation, the calculations of the buckling loads are rather simple and generally may result in closed-form solutions.

Klossner and Forry [13] studied the buckling of circular plates under symmetrical temperature distribution, using by Rayleigh–Ritz method. Krizevsky and Stavsky [14] derived the equations of laminated annular plates by using Hamilton's variational principle. More advanced solutions, including transverse shear effects, have been proposed by other researchers [15–17]. Reddy and Khdeir [16] studied the buckling and free-vibration behavior of cross-ply rectangular composite laminated plates using the classical first-order and third-order plate theories under various boundary conditions. Exact analytical solutions and finite element numerical solutions were developed in their studies. They concluded that the classical plate theory overpredicts natural frequencies and buckling loads and that the difference increases by increasing the side-to-thickness ratio. Chang and Leu [17] derived a higher-order theory that accounts for transverse shear and transverse normal strains for the thermal buckling analysis of antisymmetric angle-ply laminated plates that are simply supported and subject to a uniform temperature rise. The results indicate the importance of incorporating the effect of transverse normal and shear strains in the thermal buckling analysis.

The analytical solutions for bending, buckling, natural vibration, and transient response of rectangular laminates based on the Navier and Levy solution approaches are presented in [18] for the classical and first-order shear deformation plate theories (FSDT), respectively. The novel formulation, based on the ideas of Reddy [19], has seven parameters and still satisfies the tangential traction-free conditions on the inner and outer surfaces of the shell. Several example are shown to verify the present formulation when it is compared with the first-order shear deformation shell theory also

Received 27 July 2004; accepted for publication 19 December 2006.

*Assistant Professor, Department of Mechanical Engineering; m-najafizadeh@iau-arak-ac-ir.

developed herein for isotropic and composite shells. A review of the shear deformation plate and shell theories and a consistent third-order theory for composite shells was carried out by Reddy and Arciniega [20].

Tanigawa et al. [21] derived a one-dimensional temperature solution for a nonhomogeneous plate in the transient state and optimized the material compositions by introducing a laminated composite model. The optimal composition profile problems of the FGM to decrease the thermal stresses and thermal stress intensity factor were discussed by Noda [22,23]. He concluded that when the continuously changing composition between ceramics and metals can be selected pertinently, thermal stresses in the FGM are significantly decreased.

Javaheri and Eslami [24,25] presented the thermal and mechanical buckling of rectangular FGM plates based on the classical and high-order plate theories. The buckling analysis of circular FGM plates is given by Najafizadeh and Eslami [26,27]. More recently, Ma and Wang [28] studied nonlinear bending and postbuckling of a functionally graded circular plate under mechanical and thermal loadings based on the von Kármán plate theory. The thermal and mechanical buckling of FGM circular plates based on the first-order shear deformation plate theory is studied by Najfizadeh and Hedayati [29].

In the present paper, the equilibrium and stability equations for functionally graded circular plates (FGCPs) are obtained on the basis of higher-order shear deformation plate theory (HSDT). Resulting equations are employed to obtain the closed-form solutions for the critical buckling load. To establish the fundamental system of equations for the buckling analysis, it is assumed that the nonhomogeneous mechanical properties are given by a power form of a coordinate variable z.

Functionally Graded Circular Plates

FGMs are typically made from a mixture of ceramics and metal or a combination of different metals. The ceramic constituent of the material provides the high temperature resistance due to its low conductivity. The ductile metal constituent, on the other hand, prevents fracture caused by stresses due to a high temperature gradient in a very short period of time. Further, a mixture of a ceramic and a metal with a continuously varying volume fraction can be easily manufactured.

The volume fractions of the ceramic V_c and metal V_m, corresponding to the power law, are expressed as [30]

$$V_c = \left(\frac{2z+h}{2h}\right)^n, \qquad V_m = 1 - V_c \tag{1}$$

where z is the thickness coordinate ($-h/2 \le z \le h/2$), and n is the power law index that takes values greater than or equal to zero. The variation of the composition of ceramics and metal is linear for $n = 1$. The value of $n = 0$ represents a fully ceramic plate. The mechanical properties of FGM are determined from the volume fraction of the material constituents. We assume that the nonhomogeneous material properties, such as the modulus of elasticity E, change in the thickness direction z, based on Voigt's rule over the whole range of the volume fraction [28], whereas Poisson's ratio ν is assumed to be constant [31] as

$$E = E(z) = E_c V_c + E_m(1 - V_c), \qquad \nu = \text{constant} \tag{2}$$

where the subscripts m and c refer to the metal and ceramic constituents, respectively. Substituting Eq. (1) into Eq. (2), material properties of the FGM plate are determined, which are the same as the equations proposed by Reddy and Praveen [30]

$$E = E(z) = E_m + (E_c - E_m)\left(\frac{2z+h}{2h}\right)^n, \qquad \nu = \nu_c = \nu_m \tag{3}$$

Equilibrium and Stability Equations

We initially consider a FGM circular thin flat plate of radius a and thickness h, subjected to the mechanical loads. Polar coordinates r, θ, and z are assumed for derivations. The general strain-displacement relations are [8]

$$\begin{gathered}
\epsilon_r = u_{,r} + \frac{1}{2}(w_{,r})^2, \qquad \epsilon_\theta = \frac{1}{r}v_{,\theta} + \frac{u}{r} + \frac{1}{2}\left(\frac{1}{r}w_{,\theta}\right)^2 \\
\epsilon_{r\theta} = \frac{1}{r}u_{,\theta} + v_{,r} - \frac{v}{r} + \frac{1}{r}w_{,r}w_{,\theta}, \qquad \epsilon_{rz} = u_{,z} + w_{,r} + w_{,r}w_{,z} \\
\epsilon_{\theta z} = v_{,z} + \frac{1}{r}w_{,\theta} + \frac{1}{r}w_{,\theta}w_{,z}
\end{gathered} \tag{4}$$

where ϵ_r and ϵ_θ are the normal strain; $\epsilon_{r\theta}$, ϵ_{rz}, and $\epsilon_{\theta z}$ are the shear strains; u, v, and w denote the displacement components in the r, θ, and z directions, respectively, and a comma indicates the partial derivative.

The third-order theory of Reddy [16], used in the present study, is based on the following displacement field:

$$\begin{gathered}
u(r,\theta,z) = u_0(r,\theta) + zu_1(r,\theta) + z^2u_2(r,\theta) + z^3u_3(r,\theta) \\
v(r,\theta,z) = v_0(r,\theta) + zv_1(r,\theta) + z^2v_2(r,\theta) + z^3v_3(r,\theta) \\
w(r,\theta) = w_0(r,\theta)
\end{gathered} \tag{5}$$

These equations can be reduced by satisfying the stress-free conditions on the top and bottom faces of the laminates, which are equivalent to $\epsilon_{rz} = \epsilon_{\theta z} = 0$ at $z = \pm h/2$. Thus,

$$\begin{gathered}
u = u_0 + zu_1 - \frac{4z^3}{3h^2}(u_1 + w_{0,r}) \\
v = v_0 + zv_1 - \frac{4z^3}{3h^2}(v_1 + w_{0,r}) \qquad w = w_0
\end{gathered} \tag{6}$$

Substituting Eq. (6) into the nonlinear strain-displacement relations (4) gives the kinematic relations as

$$\begin{gathered}
\begin{pmatrix}\epsilon_r\\ \epsilon_\theta\\ \epsilon_{r\theta}\end{pmatrix} = \begin{pmatrix}\epsilon_r^0\\ \epsilon_\theta^0\\ \epsilon_{r\theta}^0\end{pmatrix} + z\begin{pmatrix}k_r\\ k_\theta\\ k_{r\theta}\end{pmatrix} + z^3\begin{pmatrix}k_1\\ k_2\\ k_3\end{pmatrix} \\
\begin{pmatrix}\epsilon_{rz}\\ \epsilon_{\theta z}\end{pmatrix} = \begin{pmatrix}\epsilon_{rz}^0\\ \epsilon_{\theta z}^0\end{pmatrix} + z^2\begin{pmatrix}k_{rz}\\ k_{\theta z}\end{pmatrix}
\end{gathered} \tag{7}$$

where

$$\begin{pmatrix}\epsilon_r^0\\ \epsilon_\theta^0\\ \epsilon_{r\theta}^0\end{pmatrix} = \begin{pmatrix} u_{0,r} + \frac{1}{2}w_{0,r}^2 \\ \frac{u_0}{r} + \frac{1}{r}v_{0,\theta} + \frac{1}{2}\left(\frac{1}{r}w_{0,r}\right)^2 \\ \frac{1}{r}u_{0,\theta} + v_{0,r} - \frac{v_0}{r} + \frac{1}{r}w_{0,r}.w_{0,\theta}\end{pmatrix}$$

$$\begin{pmatrix}k_r\\ k_\theta\\ k_{r\theta}\end{pmatrix} = \begin{pmatrix} u_{1,r} \\ \frac{1}{r}v_{1,\theta} + \frac{u_1}{r} \\ \frac{1}{r}u_{1,\theta} + v_{1,r} - \frac{v_1}{r}\end{pmatrix}$$

$$\begin{pmatrix}k_1\\ k_2\\ k_3\end{pmatrix} = \begin{pmatrix} \frac{-4}{3h^2}(u_{1,r} + w_{0,rr}) \\ \frac{-4}{3h^2}\left(\frac{1}{r}v_{1,\theta} + \frac{1}{r^2}w_{0,\theta\theta} + \frac{u_1}{r} + \frac{1}{r}w_{0,rr}\right) \\ \frac{-4}{3h^2}\left(\frac{1}{r}u_{1,\theta} + \frac{2}{r}w_{0,r} + v_{1,r} - \frac{2}{r^2}w_{0,\theta} - \frac{v_1}{r}\right)\end{pmatrix}$$

$$\begin{pmatrix}\epsilon_{rz}^0\\ \epsilon_{\theta z}^0\end{pmatrix} = \begin{pmatrix} u_1 + w_{0,r} \\ v_1 + \frac{1}{r}w_{0,\theta}\end{pmatrix}, \qquad \begin{pmatrix}k_{rz}\\ k_{\theta z}\end{pmatrix} = \begin{pmatrix} \frac{-4}{h^2}(u_1 + w_{0,r}) \\ \frac{-4}{h^2}\left(v_1 + \frac{1}{r}w_{0,\theta}\right)\end{pmatrix} \tag{8}$$

Hooke's law for a plate is defined as

$$\sigma_r = \frac{E}{(1-\nu^2)}[\epsilon_r + \nu\epsilon_\theta], \qquad \sigma_\theta = \frac{E}{(1-\nu^2)}[\epsilon_\theta + \nu\epsilon_r]$$
$$\sigma_{r\theta} = \frac{E}{2(1+\nu)}\epsilon_{r\theta}, \qquad \sigma_{rz} = \frac{E}{2(1+\nu)}\epsilon_{rz} \qquad \sigma_{\theta z} = \frac{E}{2(1+\nu)}\epsilon_{\theta z} \tag{9}$$

The stress resultants N_i, M_i, P_i, Q_i, and R_i are expressed as

$$(N_i, M_i, P_i) = \int_{-h/2}^{h/2} \sigma_i(1, z, z^3)\,\mathrm{d}z \qquad i = r, \theta, r\theta$$
$$(Q_i, R_i) = \int_{-h/2}^{h/2} \sigma_{iz}(1, z^2)\,\mathrm{d}z \qquad i = r, \theta \tag{10}$$

Substituting Eqs. (7) and (9) into Eq. (10) gives the constitutive relations as

$$\begin{aligned}
(N_r, M_r, P_r) &= \frac{1}{(1-\nu^2)}[(A, B, D)(\epsilon_r^0 + \nu\epsilon_\theta^0) + (B, C, F) \\
&\quad \times (k_r + \nu k_\theta) + (D, F, G)(k_1 + \nu k_2)] \\
(N_\theta, M_\theta, P_\theta) &= \frac{1}{(1-\nu^2)}[(A, B, D)(\epsilon_\theta^0 + \nu\epsilon_r^0) + (B, C, F) \\
&\quad \times (k_\theta + \nu k_r) + (D, F, G)(k_2 + \nu k_1)] \\
(N_{r\theta}, M_{r\theta}, P_{r\theta}) &= \frac{1}{2(1+\nu)}[(A, B, D)\epsilon_{r\theta}^0 + (B, C, F)k_{r\theta} \\
&\quad + (D, F, G)k_3] \\
(Q_r, R_r) &= \frac{1}{2(1+\nu)}[(A, C)\epsilon_{rz}^0 + (C, F)k_{rz}] \\
(Q_\theta, R_\theta) &= \frac{1}{2(1+\nu)}[(A, C)\epsilon_{\theta z}^0 + (C, F)k_{\theta z}]
\end{aligned} \tag{11}$$

where

$$(A, B, C, D, F, G) = \int_{-h/2}^{h/2} (1, z, z^2, z^3, z^4, z^6)E(z)\,\mathrm{d}z \tag{12}$$

The total potential energy of a plate subjected to mechanical loads is defined as

$$V = U + \Omega \tag{13}$$

where U is the membrane strain energy and Ω is the potential energy of the applied loads. The strain energy of a thin plate, based on the higher-order shear deformation theory, is defined as

$$\begin{aligned}
V = \frac{1}{2}\int_0^r \int_0^{2\pi} \int_{-h/2}^{h/2} &[\sigma_r\epsilon_r + \sigma_\theta\epsilon_\theta + \sigma_{r\theta}\epsilon_{r\theta} + \sigma_{rz}\epsilon_{rz} \\
&+ \sigma_{\theta z}\epsilon_{\theta z}]r\,\mathrm{d}r\,\mathrm{d}\theta\,\mathrm{d}z - \int_0^r \int_0^{2\pi} (p_r u)r\,\mathrm{d}r\,\mathrm{d}\theta
\end{aligned} \tag{14}$$

where p_r is the radial load distributed. The equilibrium equations of the plate may be obtained by the variational approach. Substituting Eqs. (7) and (9) into Eq. (14), the strain energy components are derived. Then, by setting them into the expression for the total potential energy function (13) with the aid of the constitutive law (11) and employing the Euler equations [16], the general equilibrium equations are obtained as

$$\begin{aligned}
&N_{r,r} + \frac{1}{r}N_{r\theta,\theta} + \frac{1}{r}(N_r - N_\theta) + p_r = 0 \\
&N_{r\theta,r} + \frac{1}{r}N_{\theta,\theta} + \frac{2}{r}N_{r\theta} = 0 \\
&Q_{\theta,\theta} + \left(rQ_r\right)_{,r} - \frac{4}{h^2}[R_{\theta,\theta} + (rR_r)_{,r}] + \frac{4}{3h^2}\Big[(rP_r)_{,rr} + 2P_{r\theta,r\theta} \\
&\quad + \frac{1}{r}P_{\theta,\theta\theta}\Big] + \frac{4}{3h^2}\left(\frac{2}{r}P_{r\theta,\theta} - P_{\theta,r}\right) + (rN_{r_0}w_{0,r} + N_{r\theta_0}w_{0,\theta})_{,r} \\
&\quad + \left(\frac{1}{r}N_{\theta_0}w_{0,\theta} + N_{r\theta_0}w_{0,r}\right)_{,\theta} = 0 \\
&rQ_r + M_\theta - \frac{4}{h^2}rR_r - \frac{4}{3h^2}P_\theta - \left(rM_r - \frac{4}{3h^2}rP_r\right)_{,r} \\
&\quad - \left(M_{r\theta} - \frac{4}{3h^2}P_{r\theta}\right)_{,\theta} = 0 \\
&rQ_\theta - \frac{4}{h^2}rR_\theta + \frac{4}{3h^2}P_{r\theta} - M_{r\theta} - \left(rM_{r\theta} - \frac{4}{3h^2}rP_{r\theta}\right)_{,r} \\
&\quad - \left(M_\theta - \frac{4}{3h^2}P_\theta\right)_{,\theta} = 0
\end{aligned} \tag{15}$$

The stability equations of thin circular plates may be derived by the energy method. If V is the total potential energy of the plate, the expansion of V about the equilibrium state into the Taylor series yields

$$\Delta V = \delta V + \tfrac{1}{2}\delta^2 V + \tfrac{1}{6}\delta^3 V + \cdots \tag{16}$$

The stability of the plate in the neighborhood of the equilibrium condition may be determined by the sign of the second variation. The condition $\delta^2 V = 0$ is used to derive the stability equations for buckling problems [8]. Let us assume that $\hat{u}_i$ denotes the displacement component of the equilibrium state and $\delta\hat{u}_i$ is the virtual displacement corresponding to a neighboring state. Denoting by $\bar{\delta}$ the variation with respect to $\hat{u}_i$, the following rule, known as the Trefftz rule, is stated for the determination of the critical load. The external load acting on the original configuration is considered to be the critical buckling load if the following variational equation is satisfied:

$$\bar{\delta}(\delta^2 V) = 0 \tag{17}$$

This rule provides the governing equations that determine the critical load. Consider the state of primary equilibrium of a circular plate under thermal loading to be designated by u_0, v_0, and w_0. The displacement components of the neighboring state are

$$\begin{aligned}
\hat{u}_0 = u_0 + u_0', \qquad \hat{v}_0 = v_0 + v_0', \qquad \hat{w}_0 = w_0 + w_0' \\
\hat{u}_1 = u_1 + u_1', \qquad \hat{v}_1 = v_1 + v_1'
\end{aligned} \tag{18}$$

where u_0', v_0', w_0', u_1', and v_1' are arbitrary small increments of displacements. Substituting Eqs. (7), (9), and (18) into Eq. (14) and collecting the second-order terms, we obtain the second variational of the potential energy that, when applying the Euler equations [8], results in the stability equations as

$$
\begin{aligned}
&N_{r_1,r}+\frac{1}{r}N_{r\theta_1,\theta}+\frac{1}{r}(N_{r_1}-N_{\theta_1})=0\\
&N_{r\theta_1,r}+\frac{1}{r}N_{\theta_1,\theta}+\frac{2}{r}N_{r\theta_1}=0\\
&Q_{\theta_1,\theta}+(rQ_{r_1})_{,r}-\frac{4}{h^2}[R_{\theta_1,\theta}+(rR_{r_1})_{,r}]+\frac{4}{3h^2}\Bigg[(rP_{r_1})_{,rr}\\
&\quad+2P_{r\theta_1,r\theta}+\frac{1}{r}P_{\theta_1,\theta\theta}\Bigg]+\frac{4}{h^2}\left(\frac{2}{r}P_{r\theta_1,\theta}-P_{\theta_1,r}\right)\\
&\quad+(rN_{r_0}w'_{0,r}+N_{r\theta_0}w'_{0,\theta})_{,r}+\left(\frac{1}{r}N_{\theta_0}w'_{0,\theta}+N_{r\theta_0}w'_{0,r}\right)_{,\theta}=0\\
&rQ_{r_1}+M_{\theta_1}-\frac{4r}{h^2}R_{r_1}-\frac{4}{3h^2}P_{\theta_1}-\left(rM_{r_1}-\frac{4r}{3h^2}P_{r_1}\right)_{,r}\\
&\quad-\left(M_{r\theta_1}-\frac{4}{3h^2}P_{r\theta_1}\right)_{,\theta}=0\\
&rQ_{\theta_1}-\frac{4r}{h^2}R_{\theta_1}+\frac{4}{3h^2}P_{r\theta_1}-M_{r\theta_1}-\left(rM_{r\theta_1}-\frac{4r}{3h^2}P_{r\theta_1}\right)_{,r}\\
&\quad-\left(M_{\theta_1}-\frac{4}{3h^2}P_{\theta_1}\right)_{,\theta}=0
\end{aligned}
\tag{19}
$$

In force resultants, the subscript 1 refers to the state of stability and the subscript 0 refers to the state of equilibrium. The terms N_{r_0}, N_{θ_0}, and $N_{r\theta_0}$ are the prebuckling force resultants obtained from the linear equilibrium equations (15).

Mechanical Buckling Analysis

The initial uniform load of the plate is assumed to be $p_0 = 0$. The plate is clamped supported along the edges in bending and rigidly fixed in extension. Under these boundary conditions, the load can be uniformly raised to a final value p such that the plate buckles. To find the critical buckling load, the prebuckling mechanical forces are obtained by solving the membrane form of equilibrium equations [29] we get

$$
N_{r_0}=-p_r, N_{\theta_0}=-p_r, N_{r\theta_0}=0 \tag{20}
$$

The clamped supported boundary condition is defined as

$$
u'_0(0)=u'_1(0)=\text{finite},\qquad w'_0(a)=\frac{\mathrm{d}w'_0(0)}{\mathrm{d}r}=\frac{\mathrm{d}w'_0(a)}{\mathrm{d}r}=0 \tag{21}
$$

The stability equations (19) based on the axisymmetric conditions $\partial(\,)/\partial\theta=0$ are defined as

$$
\begin{aligned}
&\frac{\mathrm{d}N_{r_1}}{\mathrm{d}r}+\frac{1}{r}(N_{r_1}-N_{\theta_1})=0\\
&\frac{\mathrm{d}(rQ_{r_1})}{\mathrm{d}r}-\frac{4}{h^2}\frac{\mathrm{d}(rR_{r_1})}{\mathrm{d}r}+\frac{4}{3h^2}\frac{\mathrm{d}^2(rP_{r_1})}{\mathrm{d}r^2}-\frac{4}{3h^2}\frac{\mathrm{d}P_{\theta_1}}{\mathrm{d}r}\\
&\quad+\frac{d}{\mathrm{d}r}\left(rN_{r_0}\frac{\mathrm{d}w'_0}{\mathrm{d}r}\right)=0\\
&rQ_{r_1}+M_{\theta_1}-\frac{4}{h^2}rR_{r_1}-\frac{4}{3h^2}P_{\theta_1}-\frac{d}{\mathrm{d}r}\left(rM_{r_1}-\frac{4}{3h^2}rP_{r_1}\right)=0
\end{aligned}
\tag{22}
$$

Substituting Eq. (7) into Eq. (11) and the axisymmetric conditions, we have

$$
\begin{aligned}
&(N_{r_1},M_{r_1},P_{r_1})=\frac{1}{1-\nu^2}\Bigg\{(A,B,D)\left(\frac{\mathrm{d}u'_0}{\mathrm{d}r}+\nu\frac{u'_0}{r}\right)\\
&\quad+(B,C,F)\left(\frac{\mathrm{d}u'_1}{\mathrm{d}r}+\nu\frac{u'_1}{r}\right)-\frac{4}{3h^2}(D,F,G)\Bigg[\frac{\mathrm{d}u'_1}{\mathrm{d}r}+\frac{\mathrm{d}^2w'_0}{\mathrm{d}r^2}\\
&\quad+\nu\left(\frac{u'_1}{r}+\frac{1}{r}\frac{\mathrm{d}w'_0}{\mathrm{d}r}\right)\Bigg]\Bigg\}\\
&(N_{\theta_1},M_{\theta_1},P_{\theta_1})=\frac{1}{1-\nu^2}\Bigg\{(A,B,D)\left(\frac{u'_0}{r}+\nu\frac{\mathrm{d}u'_0}{\mathrm{d}r}\right)+(B,C,F)\\
&\quad\times\left(\frac{u'_1}{r}+\nu\frac{\mathrm{d}u'_1}{\mathrm{d}r}\right)-\frac{4}{3h^2}(D,F,G)\Bigg[\frac{u'_1}{r}+\frac{1}{r}\frac{\mathrm{d}w'_0}{\mathrm{d}r}\\
&\quad+\nu\left(\frac{\mathrm{d}u'_1}{\mathrm{d}r}+\frac{\mathrm{d}^2w'_0}{\mathrm{d}r^2}\right)\Bigg]\Bigg\}\\
&(Q_{r_1},R_{r_1})=\frac{1}{2(1+\nu)}\Bigg[(A,C)\left(u'_1+\frac{\mathrm{d}w'_0}{\mathrm{d}r}\right)-\frac{4}{h^2}(C,F)\\
&\quad\times\left(u'_1+\frac{\mathrm{d}w'_0}{\mathrm{d}r}\right)\Bigg](N_{r\theta_1},M_{r\theta_1},P_{r\theta_1},Q_{\theta_1},R_{\theta_1})=0
\end{aligned}
\tag{23}
$$

Substituting Eqs. (23) into Eqs. (22),

$$
\begin{aligned}
&A'\left(\frac{\mathrm{d}^2u'_0}{\mathrm{d}r^2}+\frac{1}{r}\frac{\mathrm{d}u'_0}{\mathrm{d}r}-\frac{u'_0}{r^2}\right)+(B'+D_1)\left(\frac{\mathrm{d}^2u'_1}{\mathrm{d}r^2}+\frac{1}{r}\frac{\mathrm{d}u'_1}{\mathrm{d}r}-\frac{u'_1}{r^2}\right)\\
&\quad+D_1\left(\frac{\mathrm{d}^3w'_0}{\mathrm{d}r^3}+\frac{1}{r}\frac{\mathrm{d}^2w'_0}{\mathrm{d}r^2}-\frac{1}{r}\frac{\mathrm{d}w'_0}{\mathrm{d}r}\right)=0\\
&G_2\nabla^4w'_0-D_1\left(\frac{\mathrm{d}^3u'_0}{\mathrm{d}r^3}+\frac{2}{r}\frac{\mathrm{d}^2u'_0}{\mathrm{d}r^2}-\frac{1}{r^2}\frac{\mathrm{d}u'_0}{\mathrm{d}r}+\frac{u'_0}{r^3}\right)+(F_1+G_2)\\
&\quad\times\left(\frac{\mathrm{d}^3u'_1}{\mathrm{d}r^3}+\frac{2}{r}\frac{\mathrm{d}^2u'_1}{\mathrm{d}r^2}-\frac{1}{r^2}\frac{\mathrm{d}u'_1}{\mathrm{d}r}+\frac{u'_1}{r^3}\right)+A_1\left(\frac{\mathrm{d}u'_1}{\mathrm{d}r}+\frac{u'_1}{r}\right)\\
&\quad+(A_1+N_{r_0})\left(\frac{\mathrm{d}^2w'_0}{\mathrm{d}r^2}+\frac{1}{r}\frac{\mathrm{d}w'_0}{\mathrm{d}r}\right)=0\\
&-(B'+D_1)\left(\frac{\mathrm{d}^2u'_0}{\mathrm{d}r^2}+\frac{1}{r}\frac{\mathrm{d}u'_0}{\mathrm{d}r}-\frac{u'_0}{r^2}\right)-C_1\left(\frac{\mathrm{d}^2u'_1}{\mathrm{d}r^2}+\frac{1}{r}\frac{\mathrm{d}u'_1}{\mathrm{d}r}-\frac{u'_1}{r^2}\right)\\
&\quad+(F_1+G_2)\left(\frac{\mathrm{d}^3w'_0}{\mathrm{d}r^3}+\frac{1}{r}\frac{\mathrm{d}^2w'_0}{\mathrm{d}r^2}-\frac{1}{r}\frac{\mathrm{d}w'_0}{\mathrm{d}r}\right)+A_1\left(u'_1+\frac{\mathrm{d}w'_0}{\mathrm{d}r}\right)=0
\end{aligned}
\tag{24}
$$

where

$$
\begin{aligned}
&A'=\frac{A}{1-\nu^2},\qquad B'=\frac{B}{1-\nu^2},\qquad C'=\frac{C}{1-\nu^2}\\
&D'=\frac{D}{1-\nu^2},\qquad F'=\frac{F}{1-\nu^2},\qquad G'=\frac{G}{1-\nu^2}\\
&D_1=-\frac{4D'}{3h^2},\qquad F_1=\frac{4F'}{3h^2},\qquad G_1=-\frac{4G'}{3h^2},\qquad G_2=\frac{4G_1}{3h^2}\\
&A_1=\frac{1}{2(1+\nu)}\left(A-\frac{8C}{h^2}+\frac{16F}{h^4}\right),\qquad C_1=C'-2F_1-G_2
\end{aligned}
\tag{25}
$$

The three Eqs. (24) can be reduced to two equations:

$$
\begin{aligned}
&-E_1\left(\frac{\mathrm{d}^2u'_1}{\mathrm{d}r^2}+\frac{1}{r}\frac{\mathrm{d}u'_1}{\mathrm{d}r}-\frac{1}{r^2}u'_1\right)-E_2\left(\frac{\mathrm{d}^2y}{\mathrm{d}r^2}+\frac{1}{r}\frac{\mathrm{d}y}{\mathrm{d}r}-\frac{1}{r^2}y\right)\\
&\quad-A_1(u'_1+y)=0\\
&E_2\left(\frac{\mathrm{d}^3u'_1}{\mathrm{d}r^3}+\frac{2}{r}\frac{\mathrm{d}^2u'_1}{\mathrm{d}r^2}-\frac{1}{r^2}\frac{\mathrm{d}u'_1}{\mathrm{d}r}-\frac{1}{r^3}u'_1\right)+E_3\left(\frac{\mathrm{d}^3y}{\mathrm{d}r^3}+\frac{1}{r}\frac{\mathrm{d}^2y}{\mathrm{d}r^2}-\frac{1}{r^2}\frac{\mathrm{d}y}{\mathrm{d}r}\right.\\
&\quad\left.-\frac{1}{r^3}y\right)+A_1\left(\frac{\mathrm{d}u'_1}{\mathrm{d}r}+\frac{1}{r}u'_1\right)+(A_1+N_{r0})\left(\frac{\mathrm{d}y}{\mathrm{d}r}+\frac{1}{r}y\right)=0
\end{aligned}
\tag{26}
$$

where

$$E_1 = \frac{(B' + D_1)^2}{A'} - C_1, \qquad E_2 = F_1 + G_2 + \frac{D_1(B' + D_1)}{A'}$$
$$E_3 = G_2 + \frac{D_1^2}{A'}, \qquad y = \frac{\mathrm{d}w_0'}{\mathrm{d}r} \tag{27}$$

Substituting the first of the stability equations (26) into the second stability equation (26), we get

$$k_1\left(\frac{\mathrm{d}^3 y}{\mathrm{d}r^3} + \frac{1}{r}\frac{\mathrm{d}^2 y}{\mathrm{d}r^2} - \frac{1}{r^2}\frac{\mathrm{d}y}{\mathrm{d}r} + \frac{1}{r^3}y\right) + k_2\left(\frac{\mathrm{d}y}{\mathrm{d}r} + \frac{1}{r}y\right) = \frac{\mathrm{d}u_1'}{\mathrm{d}r} + \frac{1}{r}u_1' \tag{28}$$

where

$$k_1 = \frac{E_1E_3 - E_2^2}{A_1(E_2 - E_1)}, \qquad k_2 = \frac{E_1N_{r_0}}{A_1(E_2 - E_1)} - 1 \tag{29}$$

Calling

$$\bar{u} = \frac{\mathrm{d}u_1'}{\mathrm{d}r} + \frac{1}{r}u_1', \qquad \bar{y} = \frac{\mathrm{d}y}{\mathrm{d}r} + \frac{1}{r}y \tag{30}$$

and substituting relations (30) into Eq. (28), we have

$$k_1\left(\frac{\mathrm{d}^2\bar{y}}{\mathrm{d}r^2} + \frac{1}{r}\frac{\mathrm{d}\bar{y}}{\mathrm{d}r}\right) + k_2\bar{y} = \bar{u} \tag{31}$$

Substituting Eq. (31) into the first of the stability equations (26), we have

$$\nabla^4\bar{y} + O_1\left(\frac{\mathrm{d}^2\bar{y}}{\mathrm{d}r^2} + \frac{1}{r}\frac{\mathrm{d}\bar{y}}{\mathrm{d}r}\right) + O_2\bar{y} = 0 \tag{32}$$

where

$$O_1 = \frac{k_2}{k_1} + \frac{E_2}{E_1k_1} + \frac{A_1k_1}{E_1}, \qquad O_2 = \frac{A_1}{k_1E_1}(k_2 + 1) \tag{33}$$

The solution of Eq. (32) is

$$\begin{aligned}\bar{y} = {} & \bar{c}_1Y_0(O_3r) + \bar{c}_2J_0(O_3r) + \bar{c}_3rY_0(O_3r)[Y_0(O_3r)J_1(O_3r) \\ & - Y_1(O_3r)J_0(O_3r)] + \bar{c}_4rJ_0(O_3r)[Y_0(O_3r)J_1(O_3r) \\ & - Y_1(O_3r)J_0(O_3r)]\end{aligned} \tag{34}$$

where J_0, J_1, Y_0, and Y_1 are Bessel functions, and O_3 is

$$O_3 = \tfrac{1}{2}\sqrt{2O_1 - 2\sqrt{O_1^2 - 4O_2}} \tag{35}$$

To simplify Eq. (34), we define the boundary conditions for $\bar{y}$. Substituting Eq. (27) into Eq. (30), we have

$$\bar{y} = \frac{\mathrm{d}^2w_0'}{\mathrm{d}r^2} + \frac{1}{r}\frac{\mathrm{d}w_0'}{\mathrm{d}r} \tag{36}$$

and the moment for a circular plate for the case of polar symmetry is

$$M = \frac{\mathrm{d}^2w_0'}{\mathrm{d}r^2} + \frac{\nu}{r}\frac{\mathrm{d}w_0'}{\mathrm{d}r} \tag{37}$$

Therefore, we can consider $\bar{y}$ as a component of moment, thus,

$$\bar{y} = \text{finite} \quad \text{at } r = 0 \tag{38}$$

Applying boundary condition (38) into Eq. (34) yields

$$\bar{c}_1 = \bar{c}_3 = \bar{c}_4 = 0 \tag{39}$$

Substituting Eqs. (30) and (39) into Eq. (34), we get

$$\frac{\mathrm{d}y}{\mathrm{d}r} + \frac{1}{r}y = \bar{c}_2J_0(O_3r) \tag{40}$$

The solution of Eq. (40) is

$$y = \int\left(\frac{\bar{c}_2}{O_3}J_1(O_3r) + \frac{\bar{c}_5}{r}\right)\mathrm{d}r + \bar{c}_6 \tag{41}$$

Applying boundary conditions (21) into Eq. (41), we obtain

$$\bar{c}_5 = 0 \quad \text{at } r = 0 \qquad J_1(O_3a) = 0 \quad \text{at } r = a \tag{42}$$

The first zero of the Bessel function of first kind and first order yields

$$O_3a = 3.831 \tag{43}$$

Substituting Eqs. (20), (27), (29), (33), and (35) into Eq. (43) gives

$$\begin{aligned}N_{r_0} = {} & -\frac{(E_3E_1 - E_2^2)(7.662/a)^4}{4(4A_1 - (7.662/a)^2E_1)} \\ & + \frac{A_1(E_1 - 2E_2 + E_3)}{4A_1 - (7.662/a)^2E_1}\left(\frac{7.662}{a}\right)^2\end{aligned} \tag{44}$$

From Eqs. (12), (20), and (44), the critical buckling load of the clamped plate reduces to

$$p_{\mathrm{cr}} = \frac{58.706\zeta(\bar{h})}{\mu(\bar{h})} \tag{45}$$

where

$$\begin{aligned}\bar{h} = h/a, \qquad \mu(\bar{h}) = 4(4A_1 - 58.706E_1) \\ \zeta(\bar{h}) = 58.707(E_1E_3 - E_2^2) - 4A_1(E_1 - 2E_2 + E_3)\end{aligned} \tag{46}$$

The solution of the critical buckling load p_{cr} of FGCPs under uniform compression load based on HSDT has been obtained. The parameters ζ and μ are functions of h/a and n and are defined in the Eq. (46).

Table 1 Critical buckling loads (N/m) of FGCPs under radial compression due to HSDT (*H*), FSDT(*F*), and CPT (*C*) with respect to *n* and *h*/*a*

h/a	$H\ (n=0)$	$F\ (n=0)$	$C\ (n=0)$	$H\ (n=0.5)$	$F\ (n=0.5)$	$C\ )$ $(n=0.5)$
0.01	510,508	510,705	510,842	330,950	331,070	331,149
0.02	4,078,940	4,082,349	4,086,739	2,644,684	2,646,660	2,649,195
0.03	13,737,672	13,759,452	13,792,747	8,909,454	8,921,812	8,941,033
0.04	32,468,437	32,553,878	32,693,919	21,064,669	21,112,696	21,193,561
0.05	63,178,122	63,428,966	63,855,311	41,007,039	41,147,422	41,393,674
0.06	108,675,864	109,284,203	110,341,978	70,577,361	70,917,116	71,528,270
0.07	171,651,827	172,940,592	175,218,974	111,548,163	112,267,362	11,358,4243
0.08	254,657,974	257,126,889	261,551,355	165,612,352	166,990,095	169,548,492
0.09	360,091,111	364,466,809	372,404,175	234,373,029	236,816,003	241,407,911
0.1	490,178,407	497,467,361	510,842,490	319,334,572	323,407,504	331,149,398

Table 2 Critical buckling loads (N/m) of FGCPs under radial compression due to HSDT (H), FSDT(F), and CPT (C) with respect to n and h/a

h/a	H ($n=2$)	F ($n=2$)	C ($n=2$)	H ($n=5$)	F ($n=5$)	C ($n=5$)
0.01	198,566	198,642	198,688	167,898	167,978	168,025
0.02	1,586,726	1,588,049	1,589,506	1,341,109	1,342,718	1,344,202
0.03	5,435,084	5,353,536	5,364,582	4,514,582	4,525,432	4,536,682
0.04	12,636,405	12,669,575	12,716,048	10,662,771	10,706,302	10,753,616
0.05	24,597,056	24,694,498	24,836,032	20,729,943	20,859,122	21,003,157
0.06	42,328,863	42,565,362	42,916,663	35,621,137	35,936,128	36,293,456
0.07	66,891,504	67,393,010	68,150,072	56,193,939	56,863,074	5,763,266
0.08	99,295,554	100,257,375	10,172,838	83,251,244	84,534,600	8,602,893
0.09	140,496,263	142,203,069	144,843,739	117,535,092	119,809,945	122,490,414
0.1	191,388,144	194,235,302	198,688,257	159,721,685	163,509,043	168,025,260

Results

To illustrate the proposed approach, a ceramic/metal FGCP is considered. The combination of materials consists of aluminum and alumina. Young's modulus and Poisson's ratio for aluminum are $E_m = 70$ GPa and $\nu_m = 0.3$ and for alumina are $E_c = 380$ GPa and $\nu_c = 0.3$. Note that Poisson's ratio is selected to be constant and equal to 0.3. Variation of the critical buckling load p_{cr} vs the ratio h/a and volume fraction n are listed in Tables 1 and 2. In each table, the values of the critical buckling loads p_{cr} obtained by the method developed in the present paper, based on HSDT, are compared with respective values obtained based on FSDT and CPT [29]. These tables show that the critical buckling load increases with the increase of the ratio h/a and decreases with increase of the power law index n.

The critical buckling loads obtained based on FSDT and CPT are noticeably greater than values obtained based on HSDT. The differences are considerable for thick plates.

Figures 1 and 2 show the critical buckling load p_{cr} vs thickness of the plate for the case of uniform radial compression with clamped edge support. It is seen that the buckling load increases with the increase of thickness of the plate. It is interesting to note that the buckling load for isotropic material, where $n = 0$, is higher than that for the FGM plate. For this case, the material properties become full ceramic, and because the value of Young's modulus is much greater than the value of metal, the critical buckling load becomes considerably higher than for the case in which $n > 0$. Thus, the mechanical instability of the FGM plate is lower than that for the fully ceramic plate, for which $n = 0$. Figures 3 and 4 show case p_{cr} vs the volume fraction n. It is further shown that the buckling load decreases by the increase of volume fractions n. From Eq. (45), we conclude that the buckling load increases by the increase of the aspect ratio h/a.

In Figs. 5 and 6, buckling results for FGCPs based on HSDT are compared with results based on FSDT and CPT. Figures 5 and 6 show that increasing the ratio h/a causes the difference between HSDT results and other methods. This issue is because of considering the shear deformation of plate. Furthermore, it is clear that the higher-order method is more exact than the CPT and FSDT methods.

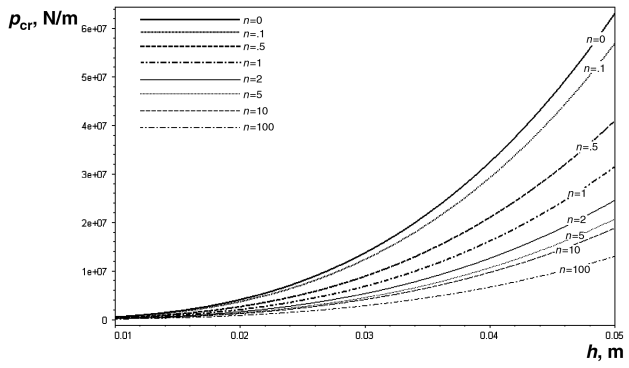

Fig. 1 Buckling load vs thickness of the plate for clamped edges and for various values of volume fraction exponent n based on HSDT.

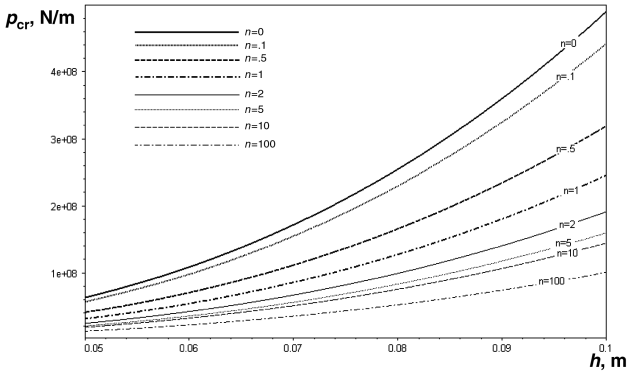

Fig. 2 Buckling load vs thickness of the plate for clamped edges and for various values of volume fraction exponent n based on HSDT.

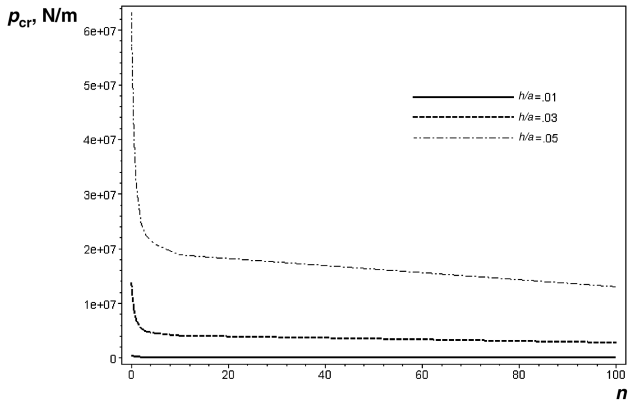

Fig. 3 Buckling load vs volume fraction exponent n for clamped edges and for various values of aspect ratio.

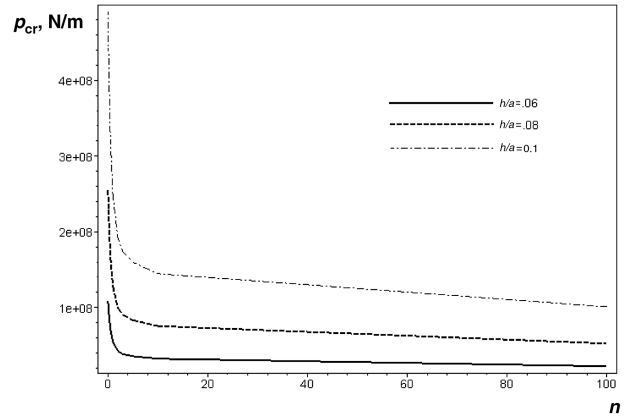

Fig. 4 Buckling load vs volume fraction exponent n for clamped edges, and for various values of aspect ratio.

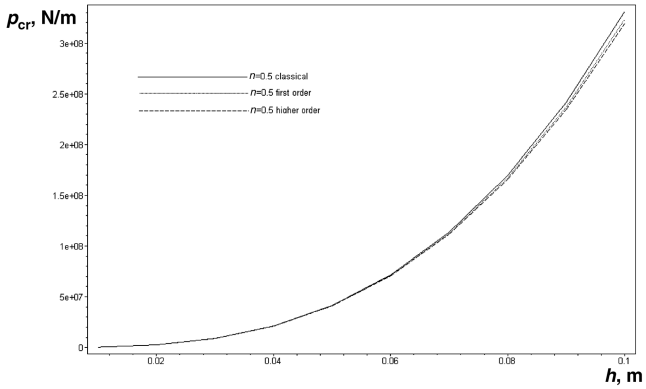

Fig. 5 Comparison of critical buckling load vs thickness of the plate for clamped edges and for various values of volume fraction *n* due to HSDT, FSDT, and CPT.

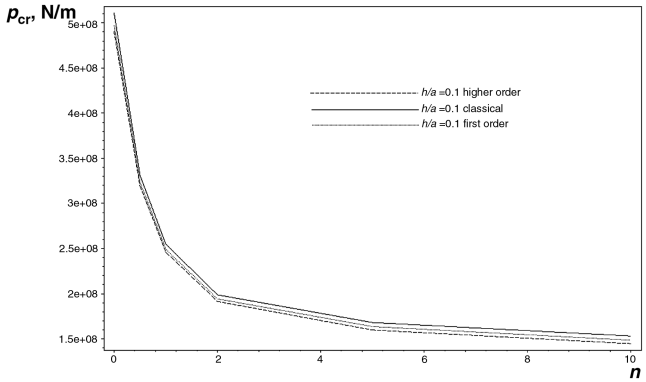

Fig. 6 Comparison of critical buckling load vs thickness of the plate for clamped edges and for various values of volume fraction *n* due to HSDT, FSDT, and CPT.

Conclusions

Circular plates are widely used in structural design problems. When such a member is subjected to uniform radial compression, its mechanical buckling capacity is important in the design stage. For a design engineer, the closed-form solution for the buckling load of such a member is essential so that he may quickly check his design. In the present paper, equilibrium and stability equations for functionally graded circular plates under uniform radial compression are obtained using the higher-order shear deformation plate theory, with the assumption of power law composition for the constituent materials. Then, buckling analysis under mechanical load and closed-form solutions for the critical buckling loads of plates are presented. Results show that the classical plate theory consistently predicts the highest buckling load, the first-order shear deformation theory consistently predicts an intermediate level of buckling load, and the higher-order shear deformation theory consistently predicts the lowest buckling load. Moreover, the buckling load predicted by the first-order shear deformation theory is consistently midway between the buckling loads predicted by the classical plate theory and higher-order shear deformation theory. This clearly shows the effect of progressively increasing the polynomial order of the assumed transverse shear kinematics.

In conclusion, functionally graded materials may present an attractive tool for a designer. These materials can be optimized to reduce the cost and weight of structures and to tailor their properties according to design requirements. Note that the mechanical buckling capacity of the functionally graded plates is, in general, lower than those of the isotropic ceramic plates with a similar geometry.

References

[1] Suresh, S., and Mortensen, A., *Fundamentals of Functionally Graded Materials*, IOM Communications Ltd., London, 1998.

[2] Yamanouchi, M., and Koizumi, M., "Functionally Gradient Materials," *Proceedings of the First International Symposium on Functionally Gradient Materials*, Functionally Gradient Materials Forum, Tokyo, 1990.

[3] Fukui, Y., "Fundamental Investigation of Functionally Gradient Material Manufacturing System Using Centrifugal Force," *JSME International Journal*, Series 3, Vol. 34, No. 1, 1991, pp. 144–148.

[4] Reddy, J. N., and Cheng, Z. Q., "Three Dimensional Trenchant Deformations of Functionally Graded Rectangular Plates," *European Journal of Mechanics, A/Solids*, Vol. 20, No. 5, Sept.–Oct. 2001, pp. 841–855.

[5] Fuchiyama, T., Noda, N., Tsuji, T., and Obata, Y., "Analysis of Thermal Stress and Stress Intensity Factor of Functionally Gradient Materials," *Functionally Gradient Materials*, Ceramic Transactions, Vol. 34, American Ceramic Society, Westerville, OH, Dec. 1993, pp. 425–432.

[6] Nan, C. W., Yuan, R. Z., and Zhang, L. M., "The Physics of Metal/Ceramic Functionally Gradient Materials," *Functionally Gradient Materials*, Ceramic Transactions, Vol. 34, American Ceramic Society, Westerville, OH, Dec. 1993, pp. 75–82.

[7] Koizumi, M., "FGM Activities In Japan," *Composites, Part B*, Vol. 28, No. 1–2, 1997, pp. 1–4.

[8] Brush, D. O., and Almroth, B. O., "Buckling of Bars," *Plates and Shells*, McGraw–Hill, New York, 1975.

[9] Leissa, A. W., "Review of Recent Developments in Laminated Composite Plate Buckling Analysis," *Composite Material Technology–1992*, Vol. 45, American Society of Mechanical Engineers, New York, 1992, pp. 1–7.

[10] Birman, V., and Bert, C. W., "Buckling of Composite Plate and Shells Subject to Elevated Temperature," *Journal of Applied Mechanics*, Series E, Vol. 60, No. 2, June 1993, pp. 514–519.

[11] Najafizadeh, M. M., and Eslami, M. R., "Thermoelastic Stability of Orthotropic Circular Plates," *Journal of Thermal Stresses*, Vol. 25, No. 10, 2002, pp. 985–1005.

[12] Pandey, M. D., and Sherbourne, A. N., "Buckling of Anisotropic Composite Plates Under Stress Gradient," *Journal of Engineering Mechanics*, Vol. 117, No. 2, 1991, pp. 260–275.

[13] Klosner, J. M., and Forry, M. J., "Buckling of Simply Supported Plates Under Arbitrary Symmetrical Temperature Distributions," *Journal of the Aerospace Sciences*, Vol. 25, 1958, pp. 181–184.

[14] Krizevsky, G., and Stavsky, Y., "Refined Theory for Vibrations and Buckling of Laminated Isotropic Annular Plates," *International Journal of Mechanical Sciences*, Vol. 38, No. 5, 1996, pp. 539–555.

[15] Reddy, J. N., Wang, C. M., and Kitopornchi, S., "Axisymmetric Bending of Functionally Graded Circular and Annular Plates," *European Journal of Mechanics, A/Solids*, Vol. 18, 1999, pp. 185–199.

[16] Reddy, J. N., and Khdeir, A. A., "Buckling and Vibration of Laminated Composite Plate Using Various Plate Theories," *AIAA Journal*, Vol. 27, No. 12, 1989, pp. 1808–1817.

[17] Chang, J. S., and Leu, S. Y., "Thermal Buckling Analysis of Antisymmetric Angle Ply Laminates Based on a Higher Order Displacement Field," *Composites Science and Technology*, Vol. 41, No. 2, 1991, pp. 109–208.

[18] Reddy, J. N., *Mechanics of Laminated Plate and Shells. Theory and Analysis*, 2nd ed., CRC Press, Boca Raton, FL, 2004.

[19] Reddy, J. N., "A Simple Higher-Order Theory for Laminated Plates," *Journal of Applied Mechanics*, Vol. 51, 1984, pp. 745–752.

[20] Reddy, J. N., and Arciniega, R. A., "Shear Deformation Plate and Shell Theories: Stavsky to Present," *Mechanics of Advanced Materials and Structures*, Vol. 11, No. 6, 2004, pp. 535–516.

[21] Tanigawa, Y., Matsomoto, M., and Akai, T., "Optimization of Material Composition to Minimize Thermal Stresses in Nonhomogeneous Plate Subjected to Unsteady Heat Supply," *JSME International Journal, Series A (Mechanics and Material Engineering)*, Vol. 40, No. 1, 1997, pp. 84–93.

[22] Fuchiyama, T., and Noda, N., "Analysis of Thermal Stresses in a Plate of Functionally Gradient Material," *JSAE Review*, Vol. 16, No. 3, 1995, pp. 263–268.

[23] Noda, N., "Thermal Stresses in Functionally Graded Materials," *Third International Congress on Thermal Stresses*, 1999, pp. 33–38.

[24] Javaheri, R., and Eslami, M. R., "Mechanical Buckling of Functionally Graded Plate Based on Higher Order Theory," *Journal of Thermal Stresses*, Vol. 6, No. 1, 2005, pp. 76–93.

[25] Javaheri, R., and Eslami, M. R., "Thermal Buckling of Graded Plates Based on Higher Order Theory," *Journal of Thermal Stresses*, Vol. 25, No. 7, 2002, pp. 603–625.

[26] Najafizadeh, M. M., and Eslami, M. R., "First Order Theory Based Thermoelastic Stability of Functionally Graded Material Circular Plates," *AIAA Journal*, Vol. 40, No. 7, 2002, pp. 1444–1450.

[27] Najafizadeh, M. M., and Eslami, M. R., "Buckling Analysis of Circular Plates of Functionally Graded Materials Under Uniform Redial Compression," *International Journal of Mechanical Sciences*, Vol. 44, No. 12, 2002, pp. 2479–2493.

[28] Ma, L. S., and Wang, T. J., "Nonlinear Bending and Post Buckling of a Functionally Graded Circular Plate Under Mechanical and Thermal Loading," *International Journal of Solids and Structures*, Vol. 40, Nos. 13–14, 2003, pp. 3311–3330.

[29] Najafizadeh, M. M., and Hedayati, B., "Refined Theory for Thermoelastic Stability of Functionally Graded Circular Plates," *Journal of Thermal Stresses*, Vol. 27, No. 9, 2004, pp. 857–880.

[30] Reddy, J. N., and Praveen, G. N., "Nonlinear Transient Thermoelastic Analysis of Functionally Graded Ceramic-Metal Plates," *International Journal of Solids and Structures*, Vol. 35, No. 33, 1998, pp. 4467–4476.

[31] Tanigawa, Y., Morishita, H., and Ogaki, S., "Derivation of Systems of Fundamental Equations for a Three Dimensional Thermoelastic Field with Nonhomogeneous Material Properties and Its Application to a Semi-Infinite Body," *Journal of Thermal Stresses*, Vol. 22, No. 7, Oct. 1999, pp. 689–711.

B. Balachandran
Associate Editor